High-resolution observations of naturally enhanced ion acoustic lines and accompanying auroral fine structures

R. G. Michell[1] and M. Samara[1]

[1] We present observations of naturally enhanced ion acoustic lines (NEIALs) from a ground-based campaign, combining high-resolution auroral imaging with raw voltage samples from the Poker Flat Incoherent Scatter Radar. We achieved maximum time resolution (~12 ms) by employing a single beam position. Four distinct events were identified, constituting the first common-volume imager/NEIAL observations in this mode. All were associated with auroral fine structures, were short-lived, and occurred on the boundaries of dynamic, luminous features. Their presence provides further insight into in situ processes, such as enhanced wave activity, that are otherwise unobservable using ground-based instrumentation. Combined high-resolution optical and radar observations reveal the temporal development of NEIALs in relation to the dynamic auroral fine structures present. These observations indicate that NEIALs manifest with timescales of less than 50 to 100 ms, providing a specific constraint for the modeling of their generation mechanisms.

1. Introduction and Background

[2] Combined imager and radar studies with the European Incoherent Scatter (EISCAT) radars [*Blixt et al.*, 2005; *Sedgemore-Schulthess et al.*, 1999; *Ogawa et al.*, 2000; *Grydeland et al.*, 2003, 2004] have found a correlation between specific auroral forms and a unique type of backscattered radar return. These returns, termed naturally enhanced ion acoustic lines (NEIALs), were originally observed by *Foster et al.* [1988], with the Millstone Hill Incoherent Scatter Radar and subsequently seen several times with the EISCAT radars [*Rietveld et al.*, 1991; *Collis et al.*, 1991; *Rietveld et al.*, 1996; *Sedgemore-Schulthess et al.*, 1999; *Ogawa et al.*, 2000; *Grydeland et al.*, 2003, 2004; *Strømme et al.*, 2005; *Blixt et al.*, 2005; *Ogawa et al.*, 2006; *Lunde et al.*, 2007]. They have been empirically associated with ion outflow [*Ogawa et al.*, 2000], a major aspect of magnetosphere-ionosphere coupling.

[3] Thus far observations have been unable to uniquely identify the generation mechanisms of NEIALs although progress has been made toward this goal. *Grydeland et al.* [2003, 2004] used interferometry to determine that the NEIAL scattering region is localized to within a few hundred meters in the direction perpendicular to the magnetic field and that both ion acoustic shoulders can be enhanced simultaneously. *Strømme et al.* [2005] examined enhanced Langmuir waves associated with NEIALs, showing that they can result from the decay of Langmuir waves while

Sullivan et al. [2008] examined the spectral characteristics of the aurora during a NEIAL event to gain insight into the energy of the precipitating electrons.

[4] Recent theoretical and modeling efforts have refined and improved the possible mechanisms for NEIAL generation. *Bahcivan and Cosgrove* [2008] showed that enhanced ion-acoustic waves can be driven by electrostatic ion cyclotron waves, and *Kontar and Pécseli* [2005] have modeled electron beam driven enhanced Langmuir waves, which decay into ion-acoustic waves. *Daldorff et al.* [2007] modeled electron acoustic and plasma waves caused by cold electron beams, which subsequently produce asymmetric ion lines. With the increased theoretical understanding, the need for higher-resolution observations of NEIALs, and their accompanying auroral forms, has also increased in order to properly compare theory to observation. In addition, their presence leads to large errors when the normal fitting procedure is used to derive the plasma parameters from the radar spectra. Characterization of NEIALs would improve the capability of these fitting procedures during such events. They tend to occur with the most active aurora, where the plasma parameters can change rapidly. Such observations allow the precise localization of the NEIALs within the auroral structure, revealing whether they are occurring in the upward or downward current region, or on the sharp gradients between them. Also, given strong enough returns, the altitude propagation of the scattering region can be identified and tracked in the raw data.

[5] Previous raw data observations, using EISCAT [*Grydeland et al.*, 2003, 2004], have revealed that NEIALs are short-lived (typically less than a few seconds) and spatially confined (few hundred meters) in the direction per-

[1]Southwest Research Institute, San Antonio, Texas, USA.

pendicular to the magnetic field. While it is difficult to regularly save raw data from EISCAT, the Poker Flat Incoherent Scatter Radar (PFISR) has that capability built in. Preliminary work by *Michell et al.* [2009, 2008], using ground-based auroral imaging and raw PFISR data, has revealed that NEIALs occur at fairly low altitudes (150–400 km), altitude ranges on the order of 1 to 2 range gates (70–200 km), and on the edges of dynamic auroral fine structure. They were also found to occur at the poleward edge of a large-scale semisteady arc structure, showing omega band characteristics.

2. Observations

[6] The data presented here were collected during an observational campaign at Poker Flat, Alaska, from 27 February through 11 March 2008. It involved running an intensified white-light all-sky and an intensified narrow field (12° × 16°) imager. The latter was centered on the magnetic zenith and equipped with a Kodak number 32 Wratten filter to remove the slow 557.7 nm emissions and transmit the prompt blue and red ones. This filter transmits the long-lived 630.0 nm emission, but with a lifetime of around 110 s, the observation of the fast motions is not significantly affected. The narrow field imager data of fast moving structures corresponds to a near instantaneous representation of the associated precipitating electron structures. Both imagers were recording at 30 frames per second. PFISR was running a mode consisting of a long pulse (480 μs) in one beam position, located along the magnetic field-aligned direction (Az. = −154.3°, El. = 77.5°). The single beam position allows for maximum time resolution in one location. The capabilities of PFISR are such that multiple beam positions can be used in rapid succession so that when integrated over a few seconds, the data in different locations can be recorded over the same time interval. The resultant raw data saved had an interpulse period (IPP) of ~12 ms, accounting for the time needed to record noise and calibration pulses.

[7] The examination of single pulse incoherent scatter radar data is not straightforward because it represents a single sampling of a random process and therefore contains uncertainty on the order of the signal itself. Single pulses can be meaningful in situations of coherent scatter (hard target) as is the case with scattering from satellites and meteor head echoes. NEIALs are the result of "coherent-like" scatter from ordered plasma that is caused by enhanced ion acoustic waves. Since they do not represent true coherent scatter, their analysis with raw data cannot be interpreted too deeply. This does not make them unusable, for example, the raw returns allow for much more accurate timing of when NEIALs occur relative to auroral forms and they reveal the temporal evolution of the scattering region on a subsecond timescale.

[8] Four distinct NEIAL events were observed, adding new information regarding their occurrence in relation to specific auroral forms. *Blixt et al.* [2005] examined four data sets that included both NEIALs and common-volume high-resolution narrow angle optical images of the aurora (the only ones known to exist at the time). They concluded that very dynamic rayed aurora, including coronal forms known as "flaming" and "pumping" aurora, were present for all of those NEIAL observations. The four cases of *Blixt et al.* [2005] were from dayside aurora, while all four examples presented here occurred in nightside aurora. These nightside observations differ from those of *Blixt et al.* [2005] in that none were associated with flaming or pumping aurora, but rather dynamic thin auroral arc structures. Of the events presented here, NEIAL number 1 was consistent with the observations of *Michell et al.* [2009], where the enhanced returns occurred on the boundary of a thin auroral arc structure.

[9] Figure 1 shows a summary of the data associated with NEIAL number 1. Figure 1 (top left) shows the electron density at 5.5 s time resolution (calculated from the scaled received power) and the power spectral density (PSD) averaged over the altitude range of 200 to 400 km covering the same time period. The normal E region can be seen around 100 to 150 km altitude, but near 0740:20 UT there is a much stronger return at 250 to 300 km altitude, identified as NEIAL number 1. It contains returned power throughout the region between both ion acoustic peaks (±4 kHz). Figure 1 (bottom left) shows the raw radar returns, covering a period of 6 s. The intensity of the aurora inside the radar beam location, defined by the full width half maximum at 100 km altitude, is represented by the overplotted line (on a scale from 30 to 255). The returns are observed immediately adjacent to the brightening of the aurora, as evidenced by the overplotted line. The strongest returns occur before the aurora crosses into the radar beam. Figure 1 (top right) shows a series of narrow field images during this time period, illustrating the progression of the auroral structure into the radar beam. The white box near the center of the images denotes the radar beam size and location at 100 km altitude. Time is noted in white in the top right corner, which corresponds to the seconds on the raw data plot (Figure 1, bottom left). The narrow field and all-sky images have been oriented the same, with north at the top and east to the left. Figure 1 (bottom right) shows an all-sky camera image, illustrating the overall auroral context of the event. The small black dot near the center of the image denotes the location and approximate size of the radar beam mapped to 100 km altitude.

[10] It should be noted that the radar data appear to have an altitude resolution of a few kilometers, due to the sampling rate. The long pulse used in this experiment (480 μs) results in altitude smearing of about 72 km. Therefore each sample represents an average of the returns coming from a 72 km long window, with the center location used to plot the data. NEIAL returns that appear to be localized in altitude to less than 72 km are due to the high time variability of the scattering region.

[11] NEIAL number 1 and previous observations [*Michell et al.*, 2009] show NEIALs occurring in the dark region immediately adjacent to a bright dynamic auroral arc. NEIAL number 2, also from 28 February 2008, showed an unexpected variation in that the returns occurred inside the brightest region of the thin auroral arc.

[12] Figure 2 uses the same intensity scale and in the same format as Figure 1. The raw radar data cover 3 s and the returns are contained within three distinct bunches. The returns associated with NEIAL number 2 occurred exactly inside the brightest region of a thin kilometer-scale arc, which is in contrast to the returns associated with NEIAL
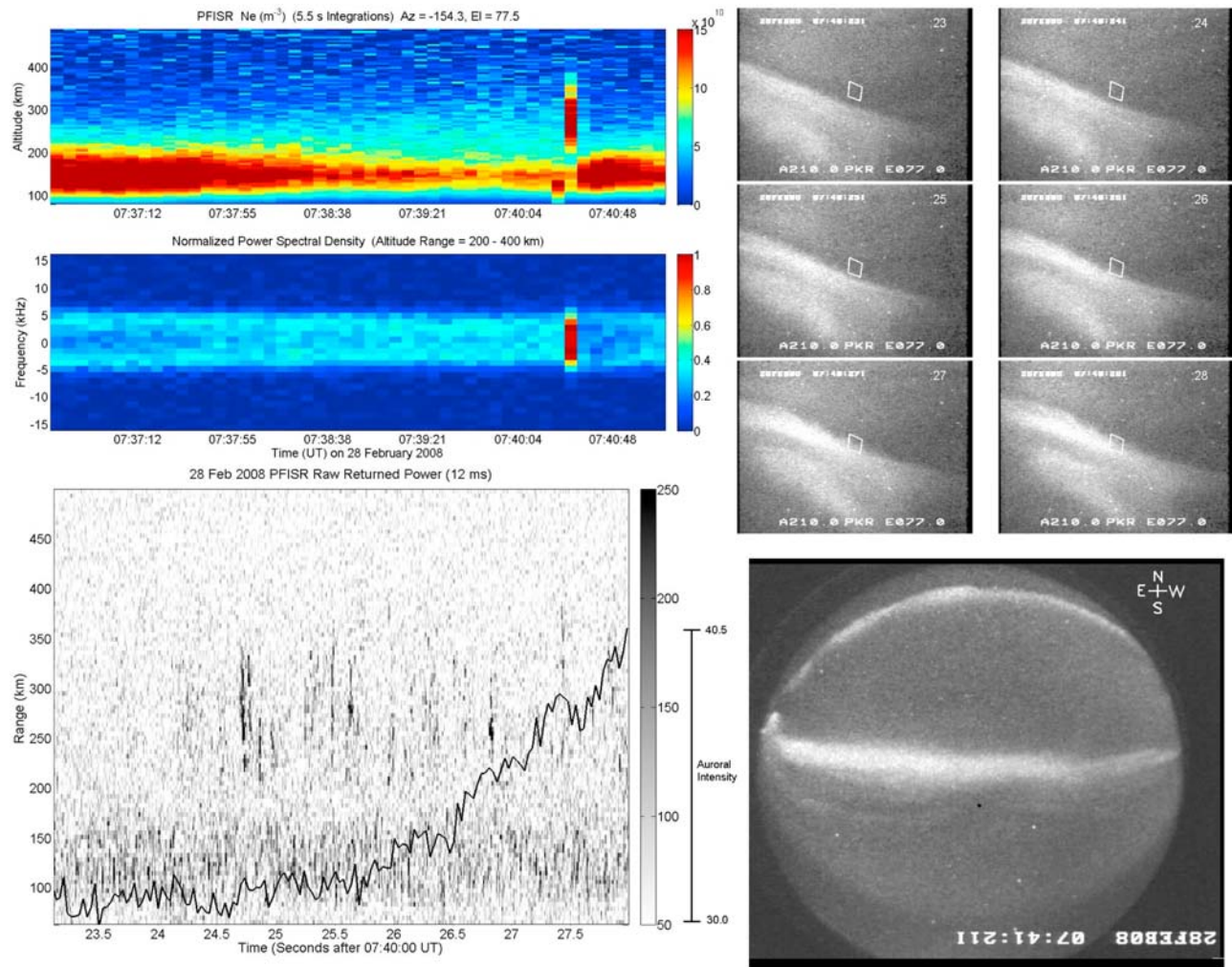
Figure 1. Summary of both (left) radar and (right) optical data. (top left) Electron density and PSD. (bottom left) The raw radar returns with the intensity of the aurora overplotted. (top right) Frames from the narrow field imager at representative times. (bottom right) All-sky camera image, showing the overall auroral context of the event. See text for more detailed descriptions of these data.

number 1. The thin arc that passes through the radar FOV is structured and dynamic, which is different from the thin arc associated with NEIAL number 1, and nearly three times as bright. The narrow field camera images from this time are spaced a half-second apart because the auroral structures were moving rapidly. These returns did not occur on a spatial gradient in intensity, but in a region where the intensity was decreasing sharply with time. The narrow field image data reveal that the thin arc was rapidly decreasing in intensity at the time of the NEIAL, so that 1 s after, the arc was completely gone.

[13] Figure 3 does not show the integrated radar data, since they are the same as in Figure 2. NEIAL number 3 is associated with a strong gradient in intensity and neither the bright or dark region. It also contains three bunches of returns, with each occurring successively higher in altitude than the previous one. The narrow field images show a thin arc structure on the edge of a larger bright region which passes through the radar beam at the time of the enhanced returns. The first two images are taken 1.0 s apart, while the rest are taken 0.2 s apart since the auroral structures were

moving very rapidly through this region. The all-sky image can be seen to differ from that in Figure 2, only 8 s earlier, showing that the whole auroral structure was very dynamic and in the midst of a poleward motion breakup.

[14] Figure 4 summarizes the radar and optical data from NEIAL number 4, which is the weakest one in the integrated data, but still fairly strong in the raw data. This is due to the returns being grouped together into two distinct bunches, with one more intense than the other. It also occurred at the edge of a thin bright arc that moved rapidly into the radar FOV. The all-sky image reveals that this NEIAL was associated with a bright, dynamic arc that was within the region of post breakup diffuse aurora.

3. Discussion

[15] The overall auroral context of these four NEIAL events can be seen to cover a range of large-scale morphologies. NEIAL number 1 occurred near the equatorward edge of a fairly stable, almost diffuse, east-west aligned arc. Examining the narrow field images, however,
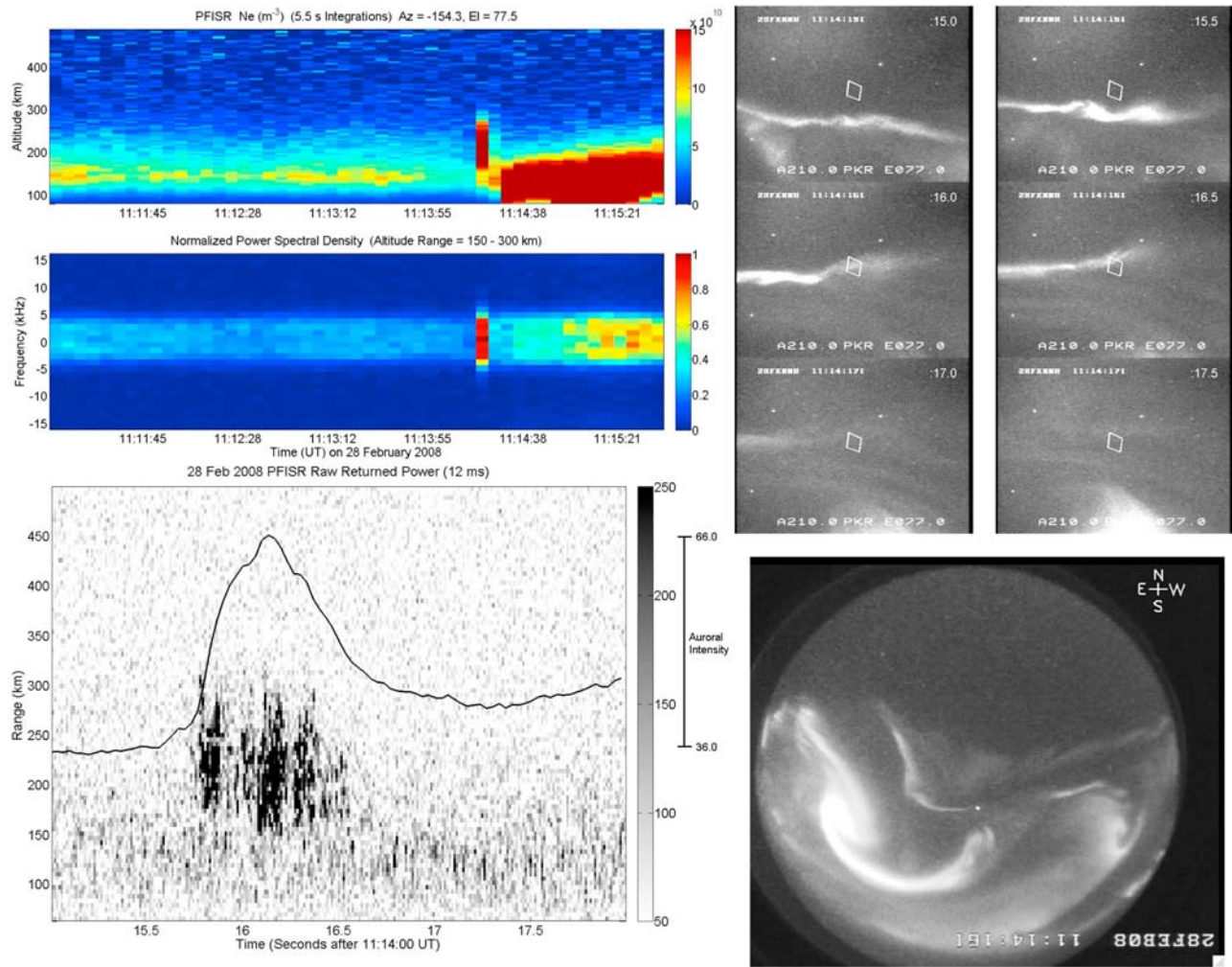
Figure 2. Radar and optical data, same format as Figure 1.

reveals small-scale structures and motions along the edge of the arc. Note that due to a data gap, the all-sky image is from nearly 1 min after the occurrence of the NEIAL, but the main arc structure and location did not change signifi- cantly during that time. The only notable change was a secondary, smaller arc that intensified in the east and propagated westward along the equatorward edge of the main arc. The NEIAL occurred when this secondary arc
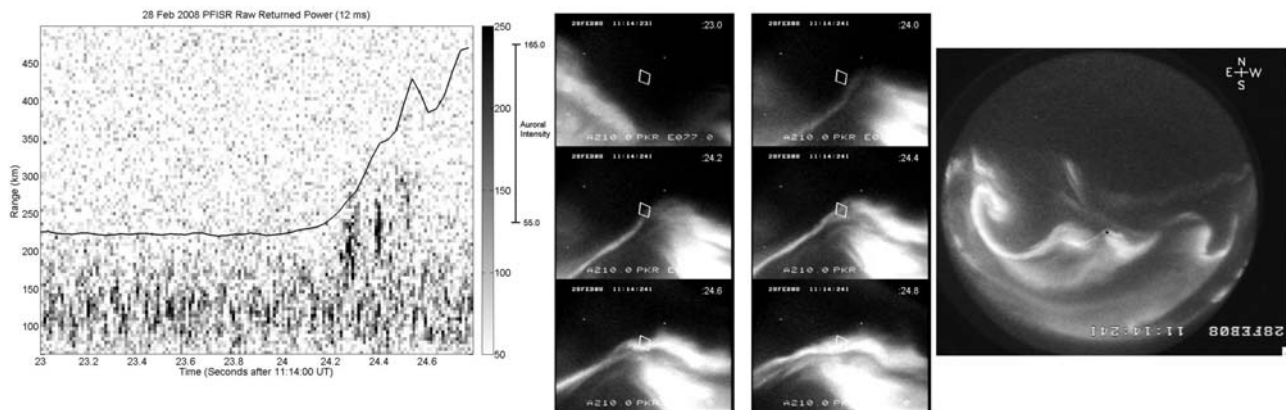

Figure 3. Radar and optical data, similar format as Figure 1, only here the integrated radar data are not shown, as it is exactly the same as in Figure 2. The radar beam location here is shown as a black dot on the all-sky image.
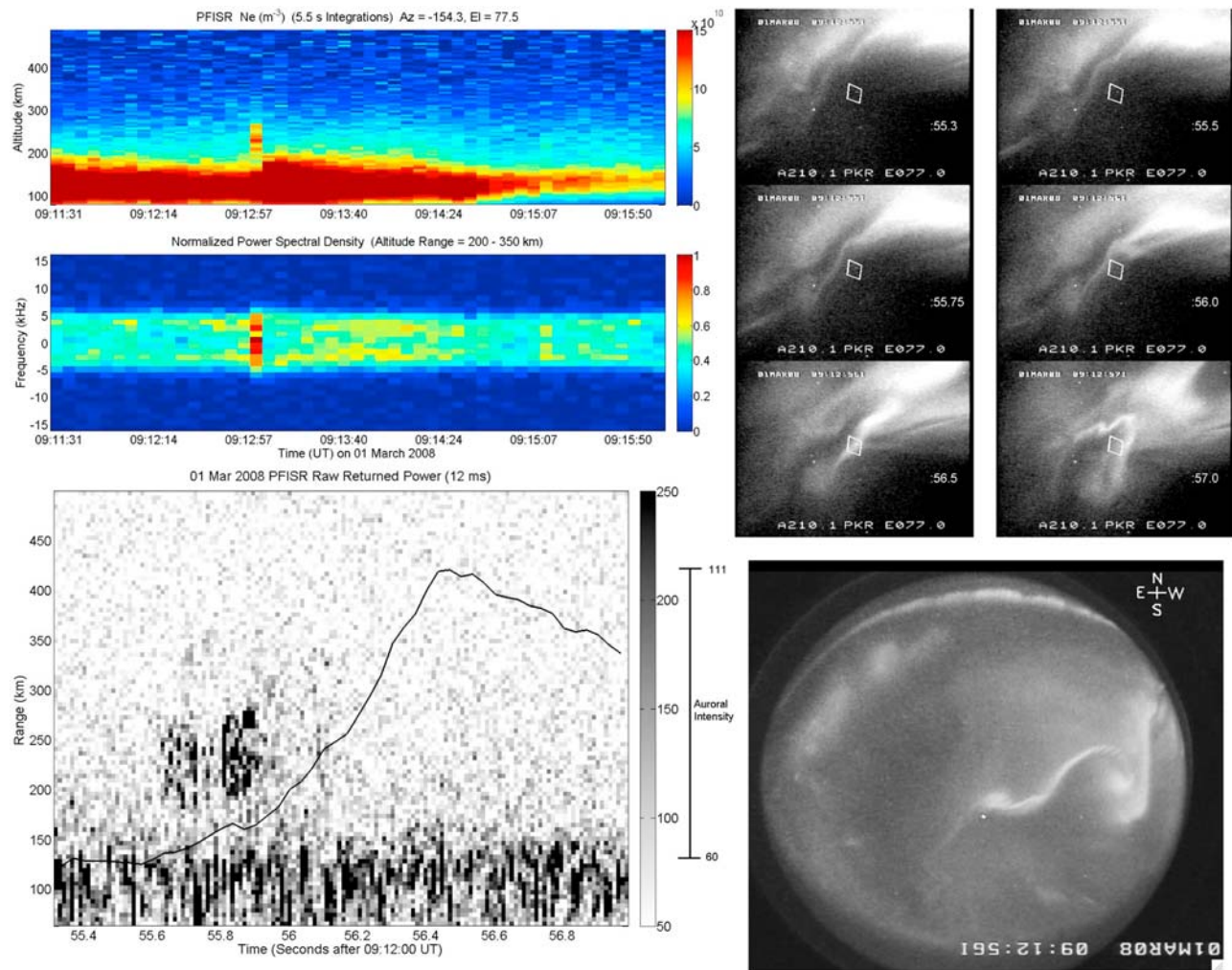
Figure 4. Radar and optical data, same format as Figure 1.

passed through the FOV of the radar, and can be seen in the narrow field images in Figure 1 (top right). Furthermore, it was associated with fine-scale ripples along the poleward edge of this secondary arc.

[16] NEIALs numbers 2 and 3 both occurred near the poleward edge of a dynamic breakup auroral arc that contained thin curtains of rays, as well as large-scale clockwise spiral features, indicative of an upward field-aligned current sheet [*Davis and Hallinan*, 1976; *Hallinan*, 1976]. NEIAL number 4, on the other hand, occurred in post breakup aurora, also associated with thin, dynamic auroral rays. The bright dynamic auroral arc can be seen far off to the north with a significant amount of diffuse aurora visible in the all-sky image. NEIAL number 4 was associated with a thin, bright and very dynamic arc structure that was embedded within that diffuse aurora.

[17] The occurrence of NEIALs, in relation to the luminous auroral features, suggests that they could be associated with both downward and upward current regions. The spectral information of the NEIAL returns can offer insight into this hypothesis. Given that NEIALs originate from current driven instabilities, it is expected that the enhanced lines should be asymmetric, with the enhancement corresponding to the direction of the current driving the instability (upward current yields enhanced upshifted shoulder while downward current yields enhanced down-shifted shoulder). Figure 5 shows the line spectra taken from the integrated radar data shown in Figures 1, 2, and 4. They are plotted on a normalized intensity scale where the black solid line is the NEIAL and the blue dotted line is the background for comparison. These spectra do not show any significant asymmetries, indicating that on a 5.5 s timescale there are enhanced ion acoustic waves traveling both toward and away from the radar. These spectra are not consistent with a current driven instability, in that there are no significant differences between the different cases, despite the different auroral context. NEIAL number 1 has symmetric shoulders and occurred in the dark region adjacent to an active arc, however NEIAL number 2 is also symmetric but occurred inside the brightest region of an active arc. NEIAL number 3 shows asymmetry, with the upshifted shoulder slightly higher than the downshifted, and it occurred on the gradient between the dark and bright regions, also not consistent with current driven instabilities. These data are more consistent with the Langmuir decay theory [*Sedgemore-Schulthess and St. Maurice*, 2001], which can
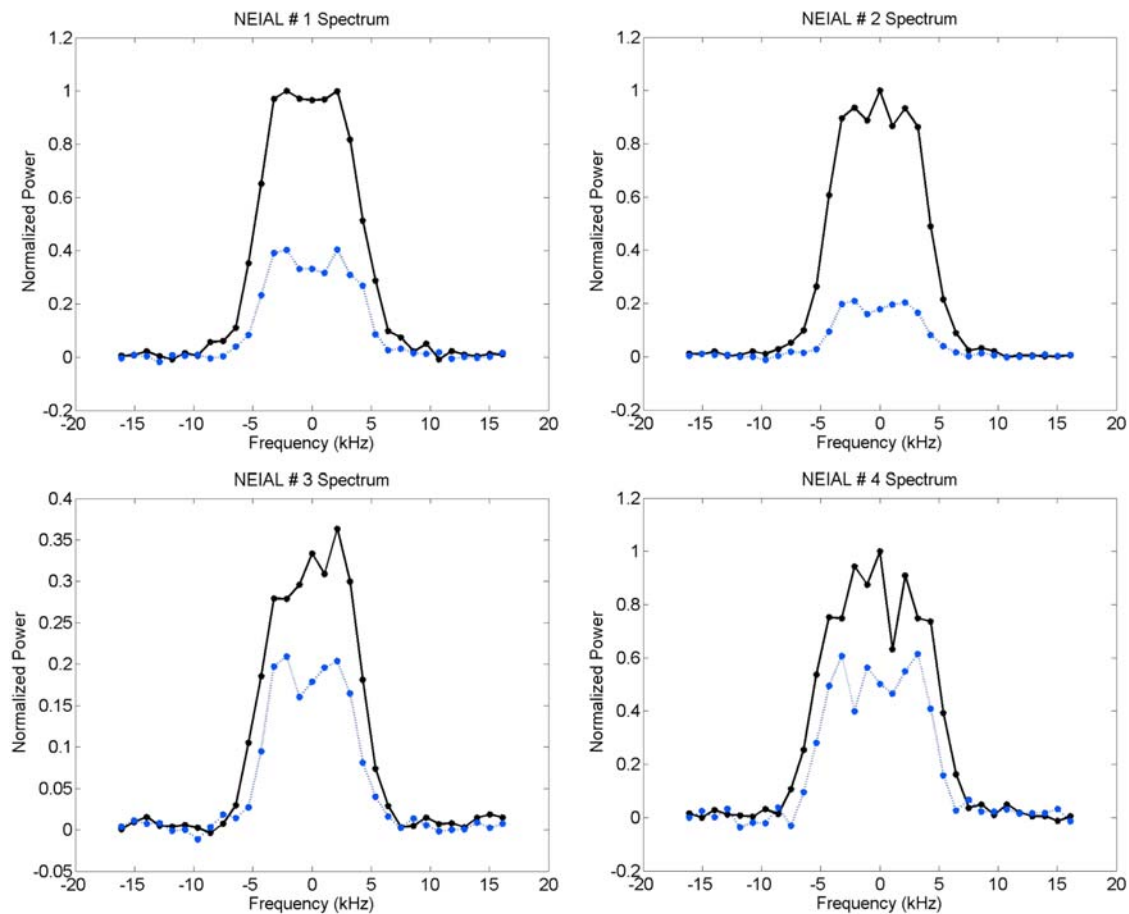
Figure 5. Spectra of the four NEIALs on a normalized intensity scale. The black solid line is the NEIAL, and the blue dotted line is a background spectra taken immediately before each NEIAL occurred. These data are for one 5.5 s integration and are averaged over the same altitude ranges shown in Figures 1, 2, and 4.

simultaneously produce symmetrically enhanced shoulders. The spectra in Figure 5 are from the integrated data. While it is possible that there are asymmetries occurring on smaller timescales that could still be consistent with current driven instabilities, given the location of the raw radar returns relative to the aurora that seems unlikely.

[18] In ISR data, zero-Doppler enhancements, also referred to as enhanced central peaks, can result from an increased ion-to-electron temperature ratio (T_i/T_e), large DC electric fields [*Raman*, 1980], as well as turbulent plasma flows and strongly varying Doppler shifts [*Knudsen et al.*, 1993]. The zero-Doppler enhancements visible in the spectra of NEIALs numbers 2, 3, and 4, shown in Figure 5, are not caused by scattering from enhanced ion acoustic waves. They occurred when the aurora moved rapidly ($\geq$2 km/s) into the radar FOV. The fast moving, small-scale auroral structures can cause a localized increase in T_i due to frictional ion heating within the region. They may also contain large-amplitude, localized electric fields [*Hallinan and Davis*, 1970], on the order of 100 mV/m for 2 km/s flows, assuming $\vec{E} = -\vec{v} \times \vec{B}$. In addition, sharply varying Doppler shifts could be present because of the rapid motion and the localized upward and downward current regions associated with the fast moving auroral structures. Therefore

the enhanced central peaks in these data are likely the result of a combination of effects from increased T_i, large electric fields and strongly varying Doppler shifts.

[19] The structure of the raw radar returns showed distinct differences. For NEIAL number 1, they were spread out sporadically over 4 s, while for NEIALs numbers 2, 3, and 4, they were bunched and clustered in less than 1 s intervals. This is an indication that the scattering regions could be narrowly localized in space, especially considering the limited extent of the associated auroral structures. This is consistent with the observations of *Grydeland et al.* [2003, 2004], who used interferometry to accurately identify the extent of the scattering region. This however does not exclude the possibility that waves with different wave numbers could exist outside of this region, as PFISR only selects waves with a specific wave number (3.0 m^{-1}).

[20] The thin auroral structures associated with NEIALs numbers 2, 3, and 4 moved rapidly through the radar beam, producing localized NEIAL signatures. However, the auroral arc associated with NEIAL number 1 moved slowly into the radar beam, therefore producing spread out and sporadic returns. It also contained fast moving ripples along its leading edge. The total power contained within NEIAL number 1 is comparable to the others and in fact larger than

that of NEIAL number 4. High-resolution examination of the auroral structures associated with NEIALs provides a means for remote sensing the localized current structures associated with the precipitating electrons. The occurrence of NEIALs appears to be intimately related to these currents systems and an understanding of this relationship will provide crucial evidence in the determination of the generation mechanisms.

[21] There are three main theories of NEIAL generation, the first is the current-driven or electron-ion two-stream instability, the second is the ion-ion two-stream instability, and the third involves nonlinear wave-wave interactions (Langmuir decay) [*Sedgemore-Schulthess and St. Maurice*, 2001]. The streaming instabilities will only produce one enhanced shoulder at a time, for a given streaming direction, while the Langmuir decay theory can enhance both simultaneously. For the current driven instability to produce both shoulders enhanced simultaneously, the current would need to flow in both directions within the scattering volume, during the NEIAL time period. Therefore constraining the timescale involved in NEIAL generation puts a limit on how fast the direction of the current changes. There are likely a number of mechanisms involved, but the times here (50 to 100 ms) are very short and it is unlikely that the current driven instabilities could be the main cause.

[22] Both the imager and radar data are accurately time-tagged with GPS, so the uncertainty in correlating them is on the order of one imager frame (33 ms). The dominant auroral lines in the fast moving structures are prompt, for example, 427.8 nm and the N_21P, resulting in near instantaneous emission after excitation. Therefore, the resulting error in the relative positioning of the aurora with the NEIALs is controlled by the relative timing errors. Given a maximum speed of the aurora of around 10 km/s, the relative positioning error is on the order of 330 m, which is significantly less than the radar beam width of 1 km.

[23] The background electron densities associated with these NEIALs can be investigated using the integrated radar data and are found to be comparable to previous observations of 5 to 30×10^{10} m^{-3} reported by *Michell et al.* [2008]. NEIAL number 1 was associated with a background electron density of 5 to 6×10^{10} m^{-3}, NEIALs numbers 2 and 3 with 4 to 5×10^{10} m^{-3}, and NEIAL number 4 with 6 to 7×10^{10} m^{-3}.

4. Conclusions

[24] To date, NEIAL observations with PFISR have been rare, and common volume auroral imaging, even more scarce. We present raw data NEIALs observed with PFISR running a single beam position for maximum time resolution. The background electron densities associated with these NEIALs are in the range of 4 to 7×10^{10} m^{-3}, which is consistent with prior observations summarized by *Michell et al.* [2008]. The raw data analysis indicates that NEIALs occur with timescales of less than 50 to 100 ms. This information can then be used to constrain the modeling of their generation mechanisms. In addition, narrow field auroral imaging shows the associated small-scale dynamic auroral structures, which offer insight into the nature, and the precise locations, of the precipitating electrons.

[25] The narrow field images reveal fine-scale auroral features (100 m scale or less) during the NEIAL events. There may be structures present that are even smaller than the resolution of the imagers used. NEIAL number 1 showed significant difference in the raw radar data signal compared to the other three NEIALs. It was sporadic and spread out in time (over ~4 s), while the rest were localized in time (≤1 s). The auroral context of NEIAL number 1 also exhibited different features both on large and small scales. NEIALs numbers 2, 3, and 4 were all associated with fast moving rayed arcs, while NEIAL number 1 was associated with "ripples" along the edge of a stable arc structure. These observations provide evidence that NEIALs are occurring in the dark regions immediately adjacent to thin bright auroral structures, however this is based on only a few examples, and many additional such examples are needed to construct a complete statistical picture. This implies that NEIALs occur within the regions of downward field-aligned current (upward moving electrons) that are paired with the strong upward currents (downward moving electrons) of the thin active auroral structures.

[26] These observations are consistent with those of *Grydeland et al.* [2003, 2004], who showed that NEIALs originate from very localized regions of space in the direction perpendicular to the magnetic field. Given more combined high-resolution imager and radar observations of NEIALs, the sizes and motions of the associated precipitation structures can be quantified in a statistical manner. This will provide insight into the relationship between current systems and NEIAL generation mechanisms. The localized nature of these returns (≤1 s) should allow ordinary incoherent scatter analysis on such active times if the raw data associated with the NEIALs are removed. Raw radar data may not be needed most of the time, but is essential during such active aurora.

References

Bahcivan, H., and R. Cosgrove (2008), Enhanced ion acoustic lines due to strong ion cyclotron wave fields, *Ann. Geophys.*, 26, 2081–2095.

Blixt, E. M., T. Grydeland, N. Ivchenko, T. Hagfors, C. La Hoz, B. S. Lanchester, U. P. Lvhaug, and T. S. Trondsen (2005), Dynamic rayed aurora and enhanced ion-acoustic radar echoes, *Ann. Geophys.*, 23, 3–11.

Collis, P. N., I. Haggstrom, K. Kaila, and M. T. Rietveld (1991), EISCAT radar observations of enhanced incoherent scatter spectra and their relation to red aurora and field-aligned currents, *Geophys. Res. Lett.*, 18, 1031–1034.

Daldorff, L. K. S., H. L. Pécseli, and J. Trulsen (2007), Nonlinearly generated plasma waves as a model for enhanced ion acoustic lines in the ionosphere, *Geophys. Res. Lett.*, 34, L18101, doi:10.1029/2007GL031513.

Davis, T. N., and T. J. Hallinan (1976), Auroral spirals: 1. Observations, *J. Geophys. Res.*, 81, 3953–3958.

Foster, J. C., C. del Pozo, K. Groves, and J.-P. Saint Maurice (1988), Radar observations of the onset of current driven instabilities in the topside ionosphere, *Geophys. Res. Lett.*, 15, 160–163.

Grydeland, T., C. La Hoz, T. Hagfors, E. M. Blixt, S. Saito, A. Strømme, and A. Brekke (2003), Interferometric observations of filamentary structures associated with plasma instability in the auroral ionosphere, *Geophys. Res. Lett.*, 30(6), 1338, doi:10.1029/2002GL016362.

Grydeland, T., E. Blixt, U. Løvhaug, T. Hagfors, C. La Hoz, and T. Trondsen (2004), Interferometric radar observations of filamented structures due to plasma instabilities and their relation to dynamic auroral rays, *Ann. Geophys.*, *22*, 1115–1132.

Hallinan, T. J. (1976), Auroral spirals: 2. Theory, *J. Geophys. Res.*, *81*, 3959–3965.

Hallinan, T. J., and T. N. Davis (1970), Small-scale auroral arc distortions, *Planet. Space Sci.*, *18*, 1735.

Knudsen, D. J., G. Haerendel, S. Buchert, M. C. Kelley, A. Steen, and U. Brandstrom (1993), Incoherent scatter radar spectrum distortions from intense auroral turbulence, *J. Geophys. Res.*, *98*, 9459–9471, doi:10.1029/93JA00179.

Kontar, E. P., and H. L. Pécseli (2005), Nonlinear wave interactions as a model for naturally enhanced ion acoustic lines in the ionosphere, *Geophys. Res. Lett.*, *32*, L05110, doi:10.1029/2004GL022182.

Lunde, J., B. Gustavsson, U. P. Løvhaug, D. A. Lorentzen, and Y. Ogawa (2007), Particle precipitations during NEIAL events: Simultaneous ground based observations at Svalbard, *Ann. Geophys.*, *25*, 1323–1336.

Michell, R. G., K. A. Lynch, C. J. Heinselman, and H. C. Stenbaek-Nielsen (2008), PFISR nightside observations of naturally enhanced ion acoustic lines, and their relation to boundary auroral features, *Ann. Geophys.*, *26*, 3623–3639.

Michell, R. G., K. A. Lynch, C. J. Heinselman, and H. C. Stenbaek-Nielsen (2009), High time-resolution PFISR and optical observations of naturally enhanced ion-acoustic lines, *Ann. Geophys.*, *27*, 1457–1467.

Ogawa, Y., R. Fujii, S. C. Buchert, S. Nozawa, S. Watanabe, and A. P. van Eyken (2000), Simultaneous EISCAT Svalbard and VHF radar observations of ion upflows at different aspect angles, *Geophys. Res. Lett.*, *27*, 81–84.

Ogawa, Y., S. C. Buchert, R. Fujii, S. Nozawa, and F. Forme (2006), Naturally enhanced ion-acoustic lines at high altitudes, *Ann. Geophys.*, *24*, 3351–3364.

Raman, R. S. V. (1980), Incoherent scattering of radar waves in the auroral ionosphere., Ph.D. thesis, Univ. of Mich., Ann Arbor.

Rietveld, M. T., P. N. Collis, and J.-P. St.-Maurice (1991), Naturally enhanced ion acoustic waves in the auroral ionosphere observed with the EISCAT 933-MHz radar, *J. Geophys. Res.*, *96*, 19,291–19,305.

Rietveld, M. T., P. N. Collis, A. P. Vaneyken, and U. P. Løvhaug (1996), Coherent echoes during EISCAT UHF Common Programmes, *J. Atmos. Terr. Phys.*, *58*, 161–174.

Sedgemore-Schulthess, F., and J.-P. St. Maurice (2001), Naturally enhanced ion-acoustic spectra and their interpretation, *Surv. Geophys.*, *22*, 55–92.

Sedgemore-Schulthess, K. J. F., M. Lockwood, T. S. Trondsen, B. S. Lanchester, M. H. Rees, D. A. Lorentzen, and J. Moen (1999), Coherent EISCAT Svalbard Radar spectra from the dayside cusp/cleft and their implications for transient field-aligned currents, *J. Geophys. Res.*, *104*, 24,613–24,624.

Strømme, A., V. Belyey, T. Grydeland, C. La Hoz, U. P. Løvhaug, and B. Isham (2005), Evidence of naturally occurring wave-wave interactions in the polar ionosphere and its relation to naturally enhanced ion acoustic lines, *Geophys. Res. Lett.*, *32*, L05103, doi:10.1029/2004GL020239.

Sullivan, J. M., M. Lockwood, B. S. Lanchester, E. P. Kontar, N. Ivchenko, H. Dahlgren, and D. K. Whiter (2008), An optical study of multiple NEIAL events driven by low energy electron precipitation, *Ann. Geophys.*, *26*, 2435.

R. G. Michell and M. Samara, Southwest Research Institute, 6220 Culebra Rd., San Antonio, TX 78238, USA. (rmichell@swri.edu)